



ELSEVIER

Journal of Organometallic Chemistry 659 (2002) 133–141

Journal
of Organo
metallic
Chemistry

www.elsevier.com/locate/jorganchem

Structure of dialkyltin diaryloxides and their reactivity toward carbon dioxide and isocyanate

Hiroyuki Yasuda, Jun-Chul Choi, Sang-Chul Lee, Toshiyasu Sakakura*

National Institute of Advanced Industrial Science and Technology (AIST), Tsukuba Central 5, Tsukuba 305-8565, Japan

Received 16 May 2002; received in revised form 3 June 2002; accepted 9 July 2002

Abstract

The synthesis, structure, and reactivity of dialkyltin diaryloxides, $R_2Sn(OAr)_2$ ($R = Me, Bu$; $Ar = Ph, p-F-C_6H_4, p-t-Bu-C_6H_4$), were investigated focusing on the differences between aryloxides and methoxides. $Me_2Sn(OAr)_2$ in the solid state formed a dimer. The aryloxo-bridged structure was confirmed by single crystal X-ray analysis. On the other hand, $R_2Sn(OAr)_2$ in solution easily dissociated upon dilution. The ^{119}Sn -NMR spectra, especially for $Me_2Sn(OAr)_2$, exhibited two distinctly resolved signals assignable to the presence of isomeric five-coordinate environments. The reactivity of $R_2Sn(OAr)_2$ was much lower than that of $R_2Sn(OMe)_2$. Thus, $R_2Sn(OAr)_2$ did not react with carbon dioxide even at high pressure and excess amount of carbon disulfide. On the other hand, the reaction with *p*-methoxyphenyl isocyanate led to the corresponding aryl carbamates, suggesting the occurrence of an isocyanate insertion into the tin–oxygen bond of $R_2Sn(OAr)_2$. © 2002 Elsevier Science B.V. All rights reserved.

Keywords: Dialkyltin diaryloxides; Carbon dioxide; Isocyanate

1. Introduction

We have recently discovered an efficient catalysis using dialkyltin dimethoxides, $R_2Sn(OMe)_2$ ($R = Bu, Me$), for the dimethyl carbonate (DMC) synthesis via the reaction of dehydrated derivatives of methanol (e.g. *ortho* esters and acetals) with carbon dioxide under supercritical conditions [1]. We have also elucidated the X-ray structure of $Me_2Sn(OMe)_2$ and its carbon dioxide insertion product, $Me_2Sn(OMe)(OCO_2Me)$, which produced DMC upon thermolysis [2]. These findings prompted us to investigate the diphenyl carbonate (DPC) synthesis catalyzed by dialkyltin diphenoxides, $R_2Sn(OPh)_2$. DPC has attracted considerable attention as a starting material of the polycarbonate synthesis by transesterification, an environmentally benign synthetic route to polycarbonates without using toxic and corrosive phosgene [3]. If dialkyltin diphenoxides catalyze the DPC formation, a key step in the catalytic cycle would be the insertion of carbon dioxide into the tin–oxygen bond. However, there have been no reports on the

reactivity of dialkyltin aryloxides with carbon dioxide, and even the structure of dialkyltin diaryloxides is not fully elucidated [4]. In this paper, we report the synthesis and structure of the dialkyltin diaryloxides, $R_2Sn(OAr)_2$ ($R = Me, Bu$; $Ar = Ph, C_6H_4-p-F, C_6H_4-p-t-Bu$), and their reactivities toward cumulenes such as carbon dioxide, carbon disulfide, and isocyanate, especially focusing on the differences between the aryloxides and methoxides.

2. Results and discussion

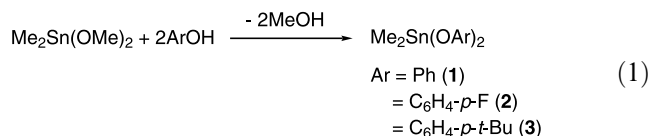
2.1. Synthesis and solid state structure of dialkyltin diaryloxides

Reaction of dimethyltin dimethoxide, $Me_2Sn(OMe)_2$, with two equivalents of phenols ($PhOH, p-F-C_6H_4OH$, and $p-t-Bu-C_6H_4OH$) at room temperature afforded the corresponding dimethyltin diaryoxide complexes ($Me_2Sn(OPh)_2$ (1), $Me_2Sn(OC_6H_4-p-F)_2$ (2), and $Me_2Sn(OC_6H_4-p-t-Bu)_2$ (3)) as white solids (Eq. (1)) [5]. Complexes 1–3 were characterized by 1H -, $^{13}C\{^1H\}$ -, and $^{119}Sn\{^1H\}$ -NMR spectroscopies, as well as elemental analysis. The ^{119}Sn -NMR spectra of 1–3 at 0.1 M in

* Corresponding author. Tel./fax: +81-298-61-4719

E-mail address: t-sakakura@aist.go.jp (T. Sakakura).

CDCl_3 contained two sharp singlets around $\delta -140$ ppm as well as one broad signal around $\delta -80$ ppm. This indicates that several species with coordination numbers around the tin atoms of four and five coexist in a dilute solution; the detailed solution structures of the dialkyltin diaryloxides are discussed in the next section.



X-ray quality crystals of **1** and **2** were obtained from a CH_2Cl_2 -ether solution at room temperature. The molecular structures of **1** and **2**, as determined by X-ray crystallography, are shown in Figs. 1 and 2, respectively; selected bond distances and angles are provided in Table 1. Note that this is the first X-ray structure of dialkyltin diaryloxides. Both complexes have a centrosymmetric aryloxo-bridged dinuclear structure. The geometry around the tin center is regarded as distorted trigonal-bipyramidal, with one of the three aryloxy groups and the two methyl groups lying on the equatorial plane and the other two aryloxy groups occupying the apical positions (e.g. O(1)–Sn(1)–O(2) bond angle for **1** of $169.95(9)^\circ$). This configuration is similar to those reported for the alkoxo- or hydroxo-bridged dinuclear trigonal-bipyramidal organotin(IV) complexes, such as $\text{Me}_2\text{Sn}(\text{OMe})_2$ [2], *i*-PrSn(O-*i*-Pr)₃ [6], $\text{Me}_2\text{Sn}(\text{OH})\text{NO}_3$ [7], *t*-Bu₂Sn(OH)X (X = F, Cl, or Br) [8], and *t*-Bu₂Sn(O₂CMe)(OH) [9]. It has been suggested, based on ¹¹⁹Sn-NMR studies, that dibutyltin diphenoxide is associated into a dimer in its saturated solution in CCl_4 or benzene [4a] or in the neat liquid [4b]. The X-ray structures of the dimethyltin diaryloxides obtained here are in accord with the dimeric structure predicted for dibutyltin diphenoxide in a concentrated solution.

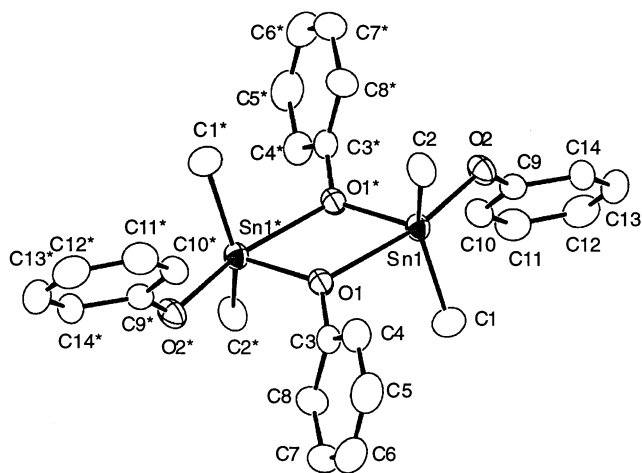


Fig. 1. ORTEP drawing of $\text{Me}_2\text{Sn}(\text{OPh})_2$ (**1**). Ellipsoids represent 50% probability.

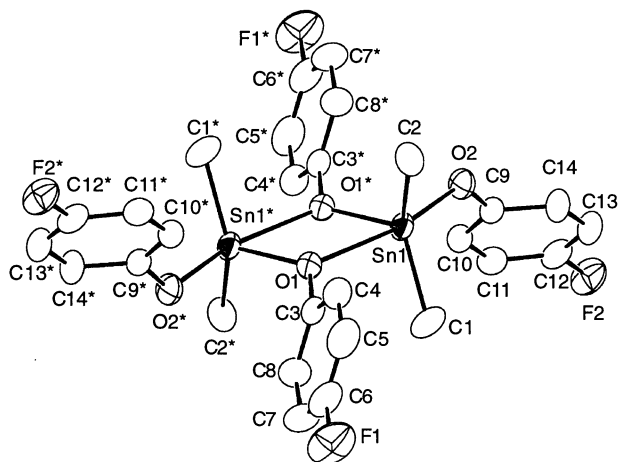


Fig. 2. ORTEP drawing of $\text{Me}_2\text{Sn}(\text{OC}_6\text{H}_4$ -*p*-F)₂ (**2**). Ellipsoids represent 50% probability.

Table 1
Selected bond distances (Å) and angles (°) for **1** and **2**

Complex 1; $\text{Me}_2\text{Sn}(\text{OPh})_2$			
<i>Bond distances</i>			
Sn(1)–O(1)	2.437(2)	Sn(1)–O(1*)	2.052(2)
Sn(1)–O(2)	2.035(2)	Sn(1)–C(1)	2.114(4)
Sn(1)–C(2)	2.095(4)	O(1)–C(3)	1.382(4)
O(2)–C(9)	1.343(4)		
<i>Bond angles</i>			
O(1)–Sn(1)–O(1*)	70.4(1)	O(1)–Sn(1)–O(2)	165.95(9)
O(1)–Sn(1)–C(1)	86.7(1)	O(1)–Sn(1)–C(2)	86.8(1)
O(1*)–Sn(1)–O(2)	95.7(1)	O(1*)–Sn(1)–C(1)	109.6(1)
O(1*)–Sn(1)–C(2)	107.3(1)	O(2)–Sn(1)–C(1)	100.1(1)
O(2)–Sn(1)–C(2)	96.2(1)	C(1)–Sn(1)–C(2)	137.6(2)
Sn(1)–O(1)–Sn(1*)	109.6(1)	Sn(1)–O(1)–C(3)	119.9(2)
Sn(1*)–O(1)–C(3)	125.8(2)	Sn(1)–O(2)–C(9)	127.0(2)
<i>Complex 2; $\text{Me}_2\text{Sn}(\text{OC}_6\text{H}_4$-<i>p</i>-F)₂</i>			
<i>Bond distances</i>			
Sn(1)–O(1)	2.409(2)	Sn(1)–O(1*)	2.061(2)
Sn(1)–O(2)	2.024(2)	Sn(1)–C(1)	2.121(4)
Sn(1)–C(2)	2.103(4)	O(1)–C(3)	1.379(4)
O(2)–C(9)	1.361(4)		
<i>Bond angles</i>			
O(1)–Sn(1)–O(1*)	69.3(1)	O(1)–Sn(1)–O(2)	163.93(9)
O(1)–Sn(1)–C(1)	86.8(1)	O(1)–Sn(1)–C(2)	87.2(1)
O(1*)–Sn(1)–O(2)	94.72(9)	O(1*)–Sn(1)–C(1)	110.3(2)
O(1*)–Sn(1)–C(2)	107.6(1)	O(2)–Sn(1)–C(1)	100.9(1)
O(2)–Sn(1)–C(2)	96.5(1)	C(1)–Sn(1)–C(2)	136.5(2)
Sn(1)–O(1)–Sn(1*)	110.7(1)	Sn(1)–O(1)–C(3)	121.7(2)
Sn(1*)–O(1)–C(3)	124.8(2)	Sn(1)–O(2)–C(9)	127.1(2)

A notable structural feature of the dimethyltin diaryloxides concerns the definite asymmetry in the aryloxo bridging. For example, the Sn(1)–O(1) distance of **1** (2.437(2) Å) is longer than the Sn(1)–O(1*) and Sn(1)–O(2) distances (2.052(2) and 2.035(2) Å, respectively). This can be accounted for by the alternating covalent/coordinate bonds in the Sn_2O_2 ring. The Sn–O covalent bond distances (Sn(1)–O(1*) and Sn(1)–O(2) for both **1** and **2**) are close to the ordinary covalent

bond of 2.06 Å [10], and lie in the range of 1.99(1)–2.097(4) Å reported for tin–aryloxy distances [11]. The Sn–O covalent bond distances in **1** and **2** are also close to those for dimethyltin dimethoxide [2]. On the contrary, slightly longer distances of Sn(1)–O(1) in **1** (2.437(2) Å) and **2** (2.409(2) Å) than the Sn(1)–O(1*) distance (2.324(6) Å) in the dimethyltin dimethoxide [2] suggest that the oxygen atoms of the aryloxides coordinate more weakly to the tin atom than the oxygen atom of the methoxide. This is probably due to the difference in the nucleophilicity of the oxygen between the aryloxy and methoxy groups. It is likely that this difference is reflected in the difference in the solution structure as well as in the reactivity toward carbon dioxide, as described in a later section.

2.2. Solution structure of dialkyltin diaryloxides

It has been revealed that dimethyltin diaryloxides have a dimeric structure in the solid state. Thus, we further investigated in detail the association of dialkyltin diaryloxides in solution. The monomers of the dialkyltin diaryloxides are distinguishable from their dimers by ^{119}Sn -NMR spectroscopy. It is known that four-coordinate dialkyltin compounds give a ^{119}Sn chemical shift (δ) ranging from about +200 to –60 ppm, whereas δ of the five-coordinate compounds ranges from –90 to –190 ppm [12]. For instance, dibutyltin dimethoxide, di-*n*-propoxide, and di-*n*-butoxide, which are suggested to be associated into a dimer (five-coordinate tin atom) based on the molecular weight and IR measurements, show δ values ranging from –159 to –165 ppm as neat liquids, whereas the neat liquid dibutyltin di-*t*-butoxide, which is fully dissociated into a monomer (four-coordinate tin atom) based on the IR, gives a low-field signal at δ –34 ppm [4a]. For the neat dibutyltin diphenoxide, $\text{Bu}_2\text{Sn}(\text{OPh})_2$ (**4**), the changes in enthalpy (ΔH) and entropy (ΔS) for the equilibrium between $[\text{Bu}_2\text{Sn}(\text{OPh})_2]_2$ and $\text{Bu}_2\text{Sn}(\text{OPh})_2$ have been estimated to be $78 \pm 2 \text{ kJ mol}^{-1}$ and $238 \pm 7 \text{ J mol}^{-1} \text{ K}^{-1}$, respectively, based on the temperature dependence (0–150 °C) of the δ values assuming δ for the dimer of –148 ppm and δ for the monomer of –48 ppm [4b].

In this study, we examined the variation with concentration in the $^{119}\text{Sn}\{^1\text{H}\}$ -NMR for **4**. The $^{119}\text{Sn}\{^1\text{H}\}$ -NMR spectrum at 0.25 M in CDCl_3 at room temperature showed one broad signal at δ –65.5 ppm (Fig. 3(a)). The broad signal remarkably shifted upfield to δ –139.0 ppm with an increase in the concentration to 3.3 M (Fig. 3(b)). Fig. 4 shows the changes in the δ values in the concentration range of 0.25–3.3 M. The δ shift clearly demonstrates that an equilibrium between four- and five-coordinate tin atoms exists in **4** in solution. It has been shown that dibutyltin dimethoxide is almost fully associated into a dimer in CCl_4 within the temperature range of ca. 20–180 °C as

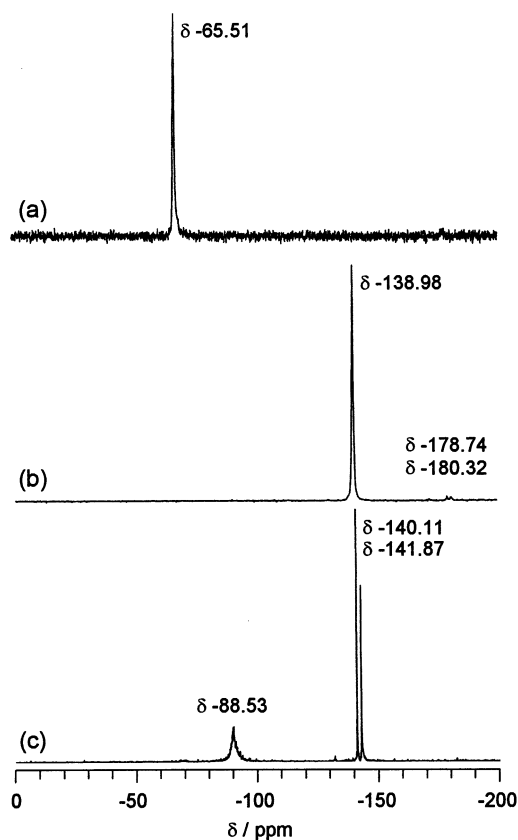


Fig. 3. $^{119}\text{Sn}\{^1\text{H}\}$ -NMR spectra of (a) $\text{Bu}_2\text{Sn}(\text{OPh})_2$ (**4**) at 0.25 M, (b) **4** at 3.3 M, and (c) $\text{Me}_2\text{Sn}(\text{OPh})_2$ (**1**) at 0.25 M in CDCl_3 at room temperature.

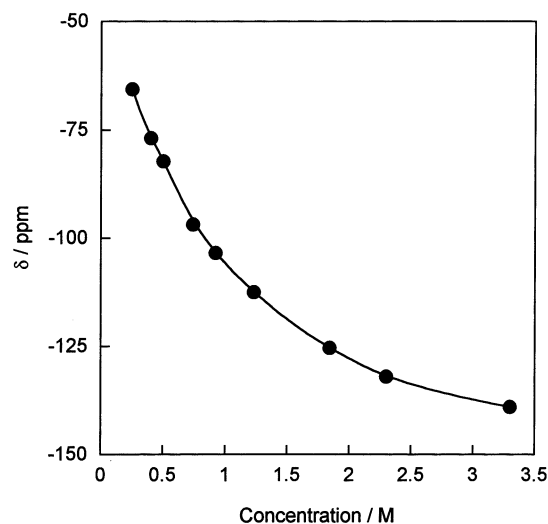


Fig. 4. Changes in the ^{119}Sn chemical shifts (δ) of $\text{Bu}_2\text{Sn}(\text{OPh})_2$ (**4**) in the concentration range of 0.25–3.3 M in CDCl_3 at room temperature.

judged by ^{119}Sn -NMR [4a]; A dimer of **4** dissociates more easily than that of dibutyltin dimethoxide does. It is noted that the $^{119}\text{Sn}\{^1\text{H}\}$ -NMR spectra of **4**, especially at high concentrations, contained two very small peaks around δ –180 ppm besides the above-stated

large broad signal, as shown in Fig. 3(b). Therefore, the structural change of **4** in solution is not so simple as was explained in the previous papers [4] based on the simple equilibrium between the dimer and the monomer.

The ^{119}Sn -NMR of $\text{Me}_2\text{Sn}(\text{OPh})_2$ (**1**) is significantly different from that of $\text{Bu}_2\text{Sn}(\text{OPh})_2$ (**4**). Fig. 3(c) shows the $^{119}\text{Sn}\{^1\text{H}\}$ -NMR spectrum of **1** at 0.25 M in CDCl_3 at room temperature. The spectrum exhibited two sharp singlets around $\delta -140$ ppm and one broad signal at $\delta -88.5$ ppm. Similarly, three signals were observed for **2** and **3**. The lower concentration caused the increase of the low-field broad signal relative to the two sharp high-field peaks. The broad signal in the intermediate region between four- and five-coordinate alkyltin compounds, are assumed to be a weighted average for more than two different species with four- or five-coordinate tin atoms, as a result of a fast equilibrium on the NMR time scale. In addition, compared with **4** more distinct appearance of two sharp singlets with the δ values in the region typical of five-coordinate alkyltin compounds suggests the presence of two kinds of magnetic environments concerning the five-coordinate tin atoms for each dimethyltin diaryloxide.

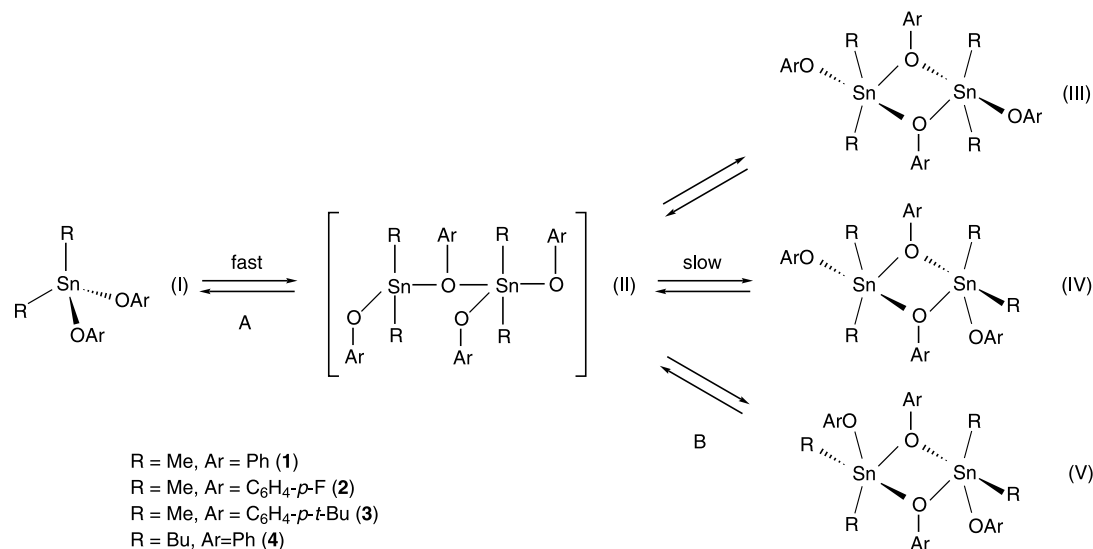
Scheme 1 depicts a plausible structural change in the dialkyltin diaryloxides to account for the ^{119}Sn -NMR results. If we assume that the bridged oxygen atoms occupy one of the two axial positions in a trigonal-bipyramid as seen in the X-ray structures (Figs. 1 and 2), three kinds of isomeric dimers ((III)–(V)) are possible. In solution, the dialkyltin diaryloxide dimer dissociates into a four-coordinate tetrahedral monomer (I), which is then in a dynamic equilibrium with each of the three dimers, (III), (IV), and (V), via the intermediate (II). For **1**–**3**, the fast equilibrium of process A would give a broad signal with the δ value belonging in the middle range of the four- and five- coordinations (ca. -80

ppm). The tin atoms in the dimers are roughly classified into two different five-coordinate magnetic environments. Thus, the rather slow equilibrium of process B would produce two distinctly resolved signals with δ values corresponding to the five coordination (ca. -140 ppm). In contrast, the two high-field signals for **4** were, if any, very small (Fig. 3(b)). This suggests that the equilibrium of process B for **4** lies further to the left compared with that for **1**–**3**. In other words, the dissociation of the dimer in solution for **4** would be easier than for the dimethyltin diaryloxides. The δ values for the dimers of **4** (ca. -180 ppm) were higher than those for the dimers of **1**–**3** (ca. -140 ppm), possibly due to the larger electron-donating property of the butyl group than the methyl group.

The results of the structural studies on **1**–**4** are summarized as follows: dialkyltin diaryloxides exist as a dimer in the solid state, while they easily dissociate into a monomer in solution. This behavior of the dialkyltin diaryloxides is in contrast to dialkyltin dimethoxide, which forms a stable dimer even in a dilute solution [2,4a]. The instability of the dialkyltin diaryloxide dimers in solution would be related to the lower nucleophilicity of the aryloxide compared with the methoxide. The reactivity of the aryloxide and methoxide toward carbon dioxide is compared in the next section.

2.3. Reactivity of dialkyltin diaryloxides with carbon dioxide and carbon disulfide

The reaction of **4** with carbon dioxide was attempted and followed by NMR spectroscopy. As mentioned in the preceding section, one broad ^{119}Sn -NMR signal was observed in the δ range from -60 to -140 ppm in the absence of carbon dioxide. When excess carbon dioxide



Scheme 1.

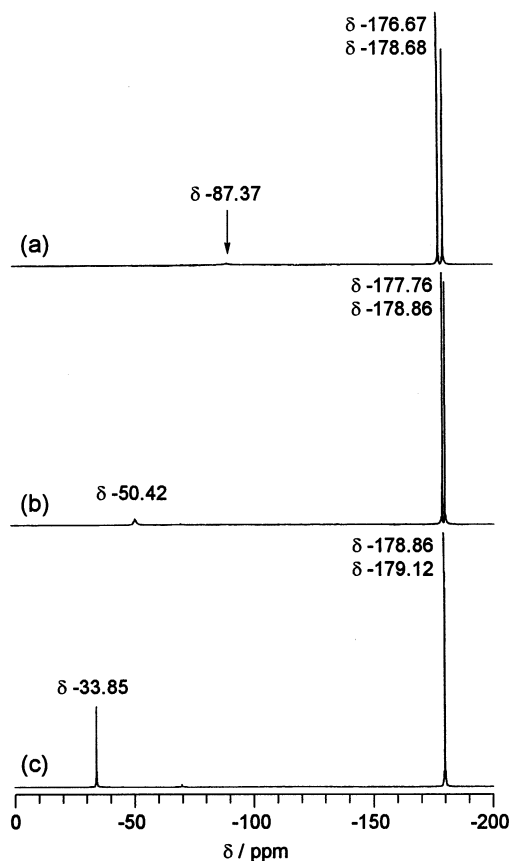


Fig. 5. $^{119}\text{Sn}\{^1\text{H}\}$ -NMR spectra of $\text{Bu}_2\text{Sn}(\text{OPh})_2$ (**4**) at 0.25 M in CDCl_3 in the presence of carbon dioxide (four equivalents) at (a) 0 °C, (b) 25 °C and (c) 60 °C.

(four equivalents) was introduced at room temperature, the two high-field singlets clearly appeared around -180 ppm while the low-field broad signal significantly decreased (Fig. 5(b)). The broad signal further decreased with decreasing the temperature (Fig. 5(a)), and completely disappeared at -50 °C. The chemical shift of the broad signal was also shifted to the higher magnetic field by lowering the temperature. However, no evidence for the insertion of carbon dioxide into the tin–oxygen bond in **4** was obtained by $^{13}\text{C}\{^1\text{H}\}$ -NMR and IR. These results suggest that the addition of carbon dioxide merely shifted the equilibrium of process B toward the five-coordinate dimers (Scheme 1). It is possible that carbon dioxide lowered the polarity of the solvent resulting in the association to the dimers, especially at lower temperatures. On the other hand, when the reaction mixture was heated to 60 °C, the low-field broad peak became sharp, showing the δ value (-33.9 ppm) assignable to the monomer (Fig. 5(c)), whereas the carbon dioxide insertion was not evidenced again by $^{13}\text{C}\{^1\text{H}\}$ -NMR. This indicates that the shift of process A to the left, that is, dissociation to the four-coordinate monomer, becomes more favorable and faster at higher temperatures. It is noteworthy that the difference in the

δ values of the two high-field singlets becomes small with increasing the temperature. Two different magnetic environments around the tin atoms in the dimers get closer at higher temperatures.

The reaction of **1** with carbon dioxide was also carried out under higher carbon dioxide pressures (80–150 atm), and followed by high-pressure IR spectroscopy. However, we could not observe the formation of the carbonate complex derived from **1** even at 150 atm; no absorption peaks assignable to $\nu(\text{CO})$ appeared in the range of 1650 – 1750 cm^{-1} . In the case of dimethyltin dimethoxide, carbon dioxide insertion into the tin–oxygen bond readily occurs at one of the two methoxy groups [2]. Therefore, it is clear that the reactivity of the dialkyltin diaryloxides with carbon dioxide is much lower than that of dimethyltin dimethoxide. Tributyltin phenoxide is also less reactive toward carbon dioxide than the alkoxide [13,14].

The reaction of **1–3** with carbon disulfide (four equivalents) was further examined at room temperature. However, no evidence for the carbon disulfide insertion into the tin–oxygen bond was obtained by NMR. The lower reactivity of the dialkyltin diaryloxides toward carbon dioxide and carbon disulfide compared with the dialkyltin dimethoxides is presumably due to the lower nucleophilicity of the aryloxy groups due to the smaller electron-donating property of the aryl groups compared with the methyl group. On the other hand, an increase in the coordination number around tin atoms by the methoxide (or aryloxy) bridging causes an increase in the electron density of the tin atoms, as evidenced by an upfield shift in the $^{119}\text{Sn}\{^1\text{H}\}$ -NMR signals for the dialkyltin diaryloxides. Since the electron-donating property of the methoxy group is higher than that of the aryloxy group, the five-coordinate dimer in solution is more stable for $\text{R}_2\text{Sn}(\text{OMe})_2$ than for $\text{R}_2\text{Sn}(\text{OAr})_2$ as discussed earlier. Moreover, the nucleophilicity of $[\text{R}_2\text{Sn}(\text{OMe})_2]_2$ is higher than that of $[\text{R}_2\text{Sn}(\text{OAr})_2]_2$ even when compared between the dimers. The higher nucleophilicity of the dimeric methoxide compared with the corresponding phenoxide is shown in the chemical shift of $^{119}\text{Sn}\{^1\text{H}\}$ -NMR: $[\text{Me}_2\text{Sn}(\text{OMe})_2]_2$ (δ -162 ppm) [2] and $[\text{Me}_2\text{Sn}(\text{OPh})_2]_2$ (δ -141 ppm). Consequently, the carbon dioxide insertion into the tin–oxygen bond might become easier in methoxides than in aryloxides.

Dialkyltin dimethoxides, $\text{R}_2\text{Sn}(\text{OMe})_2$ ($\text{R} = \text{Bu}, \text{Me}$), can efficiently catalyze the reaction of the dehydrated derivatives of methanol (e.g. *ortho* esters and acetals) with carbon dioxide to produce DMC under supercritical conditions [1]. This fact interested us in examining the catalytic efficiency of **4** for the analogous reaction of dehydrated derivatives of phenol (tetraphenoxy methane and triphenoxy methane) with carbon dioxide to produce DPC. For both reactions, however, an appreciable amount of DPC was not formed,

possibly due to no carbon dioxide insertion into the tin–oxygen bond of **4**.

2.4. Reactivity of dialkyltin diaryloxides with isocyanate

The fact that dialkyltin diaryloxides did not react with carbon dioxide and carbon disulfide induced us to further examine the reactivity of dialkyltin diaryloxides with isocyanate, which has a higher reactivity than carbon dioxide or carbon disulfide. The reaction of **4** with two equivalents of *p*-methoxyphenyl isocyanate at room temperature gave *p*-MeOC₆H₄NHCO₂Ph (**5**) in 63% yield. The structure of the carbamate **5** was confirmed by ¹H- and ¹³C{¹H}-NMR, IR, mass spectrum, and elemental analysis. Similarly, the reaction of **2** with *p*-methoxyphenyl isocyanate, followed by recrystallization from an ether–hexane solution afforded a single crystal of *p*-MeOC₆H₄NHCO₂C₆H₄-*p*-F (**6**), which was characterized by X-ray crystallography (Fig. 6 and Table 2). The unit cell contains two molecules of **6**, and the H(23) and H(24) atoms are bound to the O(5) and O(2) atoms, respectively, through a hydrogen-bond.

There is the possibility that **5** and **6** were formed via the reaction of *p*-methoxyphenyl isocyanate with ArOH (Ar = Ph, *p*-F-C₆H₄), which could be produced by the hydrolysis of **4** and **2**. Thus, the reaction of *p*-methoxyphenyl isocyanate with phenol was carried out in the absence of **4**. However, no formation of **5** was observed in this reaction, indicating tin phenoxide plays an important role in the carbamate formation. No occurrence of the reaction between phenol and phenyl

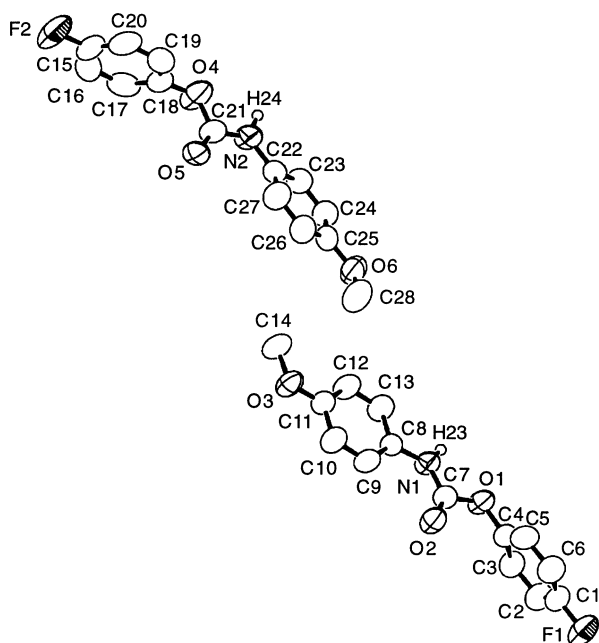


Fig. 6. ORTEP drawing of *p*-MeOC₆H₄NHCO₂C₆H₄-*p*-F (**6**). Ellipsoids represent 50% probability.

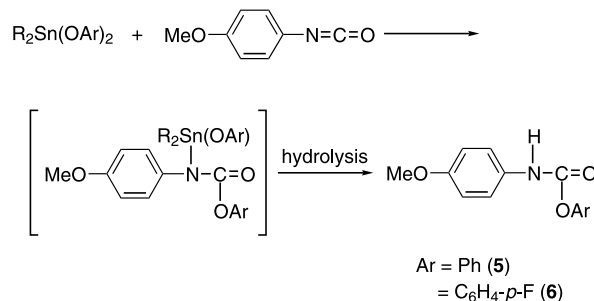
Table 2
Selected bond distances (Å) and angles (°) for **6**

Compound 6 ; <i>p</i> -MeOC ₆ H ₄ NHCO ₂ C ₆ H ₄ - <i>p</i> -F			
Bond distances			
F(1)–C(1)	1.364(4)	O(1)–C(4)	1.398(4)
O(1)–C(7)	1.375(4)	O(2)–C(7)	1.192(4)
O(3)–C(11)	1.372(4)	O(3)–C(14)	1.421(4)
N(1)–C(7)	1.341(4)	N(1)–C(8)	1.421(4)
Bond angles			
C(4)–O(1)–C(7)	118.0(3)	C(11)–O(3)–C(14)	117.6(3)
C(7)–N(1)–C(8)	126.8(3)	F(1)–C(1)–C(2)	118.3(4)
F(1)–C(1)–C(6)	119.1(4)	O(1)–C(4)–C(3)	117.6(4)
O(1)–C(4)–C(5)	120.5(4)	O(1)–C(7)–O(2)	123.1(3)
O(1)–C(7)–N(1)	107.7(3)	O(2)–C(7)–N(1)	129.1(3)
N(1)–C(8)–C(9)	124.6(3)	N(1)–C(8)–C(13)	117.1(3)
O(3)–C(11)–C(10)	117.4(3)	O(3)–C(11)–C(12)	124.8(3)

isocyanate in the absence of tributyltin phenoxide has also been pointed out [15].

If these results are taken into account, it is very probable that isocyanates such as *p*-methoxyphenyl isocyanate can insert into the tin–oxygen bond of the dialkyltin diaryloxides (Scheme 2). The formation of alkylstannylcarbamates by the insertion of isocyanates into the tin–oxygen bond of tributyltin phenoxide [15] as well as alkyltin alkoxides, such as tributyltin methoxide [15] and dibutyltin dimethoxide [16], has been assumed mainly based on IR and elemental analyses. Such alkylstannylcarbamates are readily converted into the corresponding carbamates by hydrolysis or protolysis. Thus, carbamates **5** and **6** were probably formed through hydrolysis of the tin–nitrogen bond. On the other hand, the reaction of *p*-F-C₆H₄OH with *p*-methoxyphenyl isocyanate in the presence of catalytic amount of **2** at 60 °C did not yield **6**, indicating that dialkyltin diaryloxides are not regenerated by phenolysis of alkylstannylcarbamates.

In summary, we elucidated the structure and the reactivity of the dialkyltin diaryloxides toward carbon dioxide, carbon disulfide, and isocyanate. The structure of the dimethyltin diaryloxides in the solid state determined by X-ray crystallography was aryloxy-bridged dinuclear, while the ¹¹⁹Sn-NMR spectroscopic study revealed that dialkyltin diaryloxides are easily



Scheme 2.

dissociated into a monomer when in solution. Neither carbon dioxide nor carbon disulfide reacted with the dialkyltin diaryloxides, whereas isocyanate readily reacted to produce aryl carbamates. These results clearly demonstrate that the reactivity of the dialkyltin diaryloxides is quite different from that of the dialkyltin dimethoxides.

3. Experimental

All manipulations were carried out under purified argon with use of standard Schlenk and glovebox techniques. Solvents were distilled from sodium or calcium chloride. Carbon dioxide (Showa Tansan Co., Kawasaki, purity: over 99.9%, water content: less than 0.01%) was used without further purification. Carbon disulfide and *p*-methoxyphenyl isocyanate was purchased from Tokyo Kasei Co. Dimethyltin dimethoxide [17] and dibutyltin diphenoxide (**4**) [18] were synthesized according to the literature method. Melting points (m.p.) were measured on a Yanaco Model MP-S3 melting point apparatus and are uncorrected. Elemental analyses were carried out by using a CE-EA 1110 automatic elemental analyzer. ^1H -, $^{13}\text{C}\{^1\text{H}\}$ -, and $^{119}\text{Sn}\{^1\text{H}\}$ -NMR spectra were recorded on a JEOL-LA400WB superconducting high-resolution spectrometer (400 MHz for ^1H). ^{119}Sn -NMR spectra were referenced to external tetramethyltin. IR spectra were measured on a JASCO FTIR-5300 spectrometer. IR spectra under high pressure carbon dioxide were collected by using an IR cell with zinc sulfide windows.

3.1. Synthesis of $\text{Me}_2\text{Sn}(\text{OPh})_2$ (**1**)

To a toluene (25 ml) solution of dimethyltin dimethoxide (3.3 g, 0.016 mol) was added phenol (3.0 g, 0.032 mol). After stirring the reaction mixture for 16 h at room temperature (r.t.), the solvent was evaporated. The resulting product was washed repeatedly with hexane to give a white solid. Recrystallization from a CH_2Cl_2 -ether solution gave colorless crystals of **1** (4.2 g, 79% yield). ^1H -NMR (400 MHz in CDCl_3 at 25 °C) δ 0.96 (s, 6H, CH_3 , $J(\text{Sn}-\text{C}-\text{H}) = 72.4$ Hz), 6.61–7.14 (m, 10H, aromatic). $^{13}\text{C}\{^1\text{H}\}$ -NMR (100 MHz in CDCl_3 at 25 °C) δ 2.06 (s, $\text{Sn}-\text{CH}_3$), 117.48, 120.59, 129.69, 158.50 (s, aromatic). $^{119}\text{Sn}\{^1\text{H}\}$ -NMR (149 MHz, CDCl_3 at 25 °C) δ -141.87 (s), -140.11 (s), -88.53 (br). M.p.: 166–169 °C. Anal. Calc. for $\text{C}_{14}\text{H}_{16}\text{O}_2\text{Sn}$: C, 50.20; H, 4.81. Found: C, 49.52; H, 5.06%.

3.2. Synthesis of $\text{Me}_2\text{Sn}(\text{OC}_6\text{H}_4\text{-}p\text{-F})_2$ (**2**)

Complex **2** was synthesized analogously in 82% yield as a white powder via the reaction of dimethyltin dimethoxide with two equivalents of *p*-F- $\text{C}_6\text{H}_4\text{OH}$.

^1H -NMR (400 MHz in CDCl_3 at 25 °C) δ 0.92 (s, 6H, CH_3 , $J(\text{Sn}-\text{C}-\text{H}) = 70.7$ Hz), 6.55–6.81 (m, 8H, aromatic). $^{13}\text{C}\{^1\text{H}\}$ -NMR (100 MHz in CDCl_3 at 25 °C) δ 1.98 (s, $\text{Sn}-\text{CH}_3$), 116.10 ($J(\text{C}-\text{F}) = 23.2$ Hz), 121.36, 154.98, 157.40 ($J(\text{C}-\text{F}) = 239$ Hz) (aromatic). $^{119}\text{Sn}\{^1\text{H}\}$ -NMR (149 MHz, CDCl_3 at 25 °C) δ -140.51 (s), -140.30 (s), -67.30 (br). M.p.: 234–237 °C. Anal. Calc. for $\text{C}_{14}\text{H}_{14}\text{F}_2\text{O}_2\text{Sn}$: C, 45.33; H, 3.80. Found: C, 44.88; H, 3.98%.

3.3. Synthesis of $\text{Me}_2\text{Sn}(\text{OC}_6\text{H}_4\text{-}p\text{-}t\text{-Bu})_2$ (**3**)

Complex **3** was prepared analogously by reacting dimethyltin dimethoxide with two equivalents of *p*-*t*-Bu- $\text{C}_6\text{H}_4\text{OH}$ in 76% yield as a white powder. ^1H -NMR (400 MHz in CDCl_3 at 25 °C) δ 0.93 (s, 6H, CH_3 , $J(\text{Sn}-\text{C}-\text{H}) = 71.9$ Hz), 1.25 (s, 18H, $\text{C}(\text{CH}_3)_3$), 6.52–7.10 (m, 8H, aromatic). $^{13}\text{C}\{^1\text{H}\}$ -NMR (100 MHz in CDCl_3 at 25 °C) δ 2.24 (s, $\text{Sn}-\text{CH}_3$), 31.89 (s, $\text{C}(\text{CH}_3)_3$), 34.29 (s, $\text{C}(\text{CH}_3)_3$), 120.18, 126.33, 143.06, 156.66 (s, aromatic). $^{119}\text{Sn}\{^1\text{H}\}$ -NMR (149 MHz, CDCl_3 at 25 °C) δ -144.79 (s), -141.65 (s), -75.96 (br). M.p.: 172–175 °C. Anal. Calc. for $\text{C}_{22}\text{H}_{32}\text{O}_2\text{Sn}$: C, 59.09; H, 7.21. Found: C, 58.47; H, 7.38%.

3.4. Reaction of **4** and **1** with carbon dioxide

In an NMR tube (5 mm in diameter), four equivalents of carbon dioxide (0.42 mmol) was vacuum-transferred into a CDCl_3 (0.4 ml) solution of **4** (42 mg, 0.10 mmol as a monomer). The ^1H -, $^{13}\text{C}\{^1\text{H}\}$ -, and $^{119}\text{Sn}\{^1\text{H}\}$ -NMR spectra of the reaction mixture were recorded in the temperature range from -50 to 60 °C.

A CH_2Cl_2 (4.0 ml) solution of **1** (33 mg, 0.099 mmol as a monomer) was placed in a high-pressure IR cell under argon atmosphere, followed by the introduction of carbon dioxide (1–150 atm). IR spectra from **1** were obtained by subtracting the spectrum of CH_2Cl_2 alone from the spectrum obtained for **1** in CH_2Cl_2 at each pressure.

3.5. Reaction of **1**–**3** with carbon disulfide

To a CH_2Cl_2 (5 ml) solution of **1** (0.23 g, 0.70 mmol as a monomer) was added four equivalents of carbon disulfide (0.17 ml, 2.8 mmol). After stirring the reaction mixture for 24 h at r.t., the solvent was evaporated. The resulting product was washed repeatedly with hexane to give a white solid. ^1H -, $^{13}\text{C}\{^1\text{H}\}$ -, and $^{119}\text{Sn}\{^1\text{H}\}$ -NMR data of the solid were consistent with **1**. The same result was obtained for the reaction in an NMR tube. Reactions of **2** and **3** with carbon disulfide were analogously carried out. ^1H -, $^{13}\text{C}\{^1\text{H}\}$ -, and $^{119}\text{Sn}\{^1\text{H}\}$ -NMR data of each product were consistent with those of each complex.

Table 3
Data collection and refinement parameters for **1**, **2** and **6**

	1	2	6
Formula	C ₁₄ H ₁₆ O ₂ Sn	C ₁₄ H ₁₄ F ₂ O ₂ Sn	C ₂₈ H ₂₄ F ₂ N ₂ O ₆
Formula weight	334.97	370.95	522.50
Crystal size (mm)	0.30 × 0.30 × 0.40	0.30 × 0.30 × 0.40	0.30 × 0.30 × 0.40
Crystal system	Monoclinic	Monoclinic	Triclinic
Space group	<i>P</i> 2 ₁ / <i>n</i> (No. 14)	<i>P</i> 2 ₁ / <i>n</i> (No. 14)	<i>P</i> $\bar{1}$ (No. 2)
<i>a</i> (Å)	10.354(3)	10.341(3)	10.491(1)
<i>b</i> (Å)	12.260(4)	13.045(4)	13.664(2)
<i>c</i> (Å)	11.348(3)	11.080(4)	9.852(1)
α (°)			98.89(1)
β (°)	111.29(2)	110.53(2)	105.010(10)
γ (°)			68.80(1)
<i>V</i> (Å ³)	1342.2(7)	1399.9(7)	1268.9(3)
<i>Z</i>	4	4	2
<i>T</i> (K)	296	296	296
λ (Å)	0.71069	0.71069	0.71069
<i>D</i> _{calc} (g cm ⁻³)	1.66	1.76	1.37
μ (cm ⁻¹)	18.91	18.42	1.06
<i>F</i> (000)	664	728	544
<i>R</i>	0.030	0.035	0.049
<i>R</i> _w ^a	0.041	0.053	0.069
Number of variables	155	173	344
Number of observations (<i>I</i> > 3 σ (<i>I</i>))	2430	2827	2247

$$^a w = [\sigma(F_o)]^{-2}.$$

3.6. Reaction of **4** and **2** with *p*-methoxyphenyl isocyanate

To a solution of **4** (0.21 g, 0.50 mmol) in ether (5 ml) was added two equivalents of *p*-methoxyphenyl isocyanate (0.13 ml, 0.99 mmol). When the reaction mixture was stirred at r.t., it turned into a pale yellow homogeneous solution. After 1 h, the addition of two equivalents of water (0.018 ml, 0.99 mmol) to the solution caused the instant formation of white precipitates. The precipitates were filtered, washed repeatedly with hexane, and dried in vacuo. Recrystallization from an ether–hexane solution gave 76 mg (63% yield) of colorless crystals of *p*-MeOC₆H₄NHCO₂Ph (**5**). A similar procedure employed for the reaction of **2** (0.17 g, 0.45 mmol) with *p*-methoxyphenyl isocyanate (0.12 ml, 0.93 mmol) gave *p*-MeOC₆H₄NHCO₂C₆H₄-*p*-F (**6**) (67 mg, 58% yield).

3.6.1. Compound **5**

¹H-NMR (CDCl₃, 400 MHz): δ 3.77 (s, 3H, OCH₃), 7.39–6.84 (m, 10H, aromatic and NH). ¹³C-NMR (CDCl₃, 100 MHz): δ 55.52 (OCH₃), 114.37, 120.70, 121.65, 125.60, 129.38, 130.43, 150.70, 151.95 (aromatic), 156.29 (CO). Mass spectrum (EI, 70 eV): eight most intense *m/e* peaks at 44, 66, 78, 94, 106, 121, 149, 243. IR (KBr, cm⁻¹): 1711 (ν_{CO}), 3341 (ν_{NH}). Anal. Calc. for C₁₄H₁₃NO₃: C, 69.12; H, 5.39; N, 5.76. Found: C, 69.63; H, 4.55; N, 5.51%.

3.6.2. Compound **6**

¹H-NMR (CDCl₃, 400 MHz): δ 3.77 (s, 3H, OCH₃), 7.33–6.84 (m, 9H, aromatic and NH). ¹³C-NMR (CDCl₃, 100 MHz): δ 55.80 (OCH₃), 114.67, 116.28 (*J*(C–F) = 23.1 Hz), 121.05, 123.38 (*J*(C–F) = 8.2 Hz), 130.53, 146.81 (*J*(C–F) = 1.6 Hz), 152.21, 160.43 (*J*(C–F) = 243 Hz) (aromatic), 156.64 (CO). Anal. Calc. for C₁₄H₁₂FNO₃: C, 64.36; H, 4.63; N, 5.36. Found: C, 64.76; H, 4.52; N, 5.28%.

3.7. X-ray crystallographic study

Data collection and refinement parameters for **1**, **2**, and **6** are summarized in Table 3. The data were collected on a Rigaku AFC 7R diffractometer at ambient temperature using graphite-monochromated Mo–K α radiation (0.71069 Å) and the ω scan mode ($2\theta \leq 55^\circ$). Correction for the Lorentz and polarization effects, and an empirical absorption correction (Ψ -scan) were applied. The full-matrix least-squares refinement was carried out by applying anisotropic thermal factors to all the non-hydrogen atoms. The hydrogen atoms were located by assuming an ideal geometry.

4. Supplementary material

Crystallographic data for the structural analysis of complexes **1** and **2** and compound **6** have been deposited with the Cambridge Crystallographic Data Centre

[CCDC No. 184965 (1), 184966 (2), 184967 (6)]. Copies of this information may be obtained free of charge from The Director, CCDC, 12 Union Road, Cambridge CB2 1EZ, UK (Fax: +44-1223-336033; e-mail: deposit@ccdc.cam.ac.uk or www: <http://www.ccdc.cam.ac.uk>).

References

- [1] (a) T. Sakakura, Y. Saito, M. Okano, J.-C. Choi, T. Sako, *J. Org. Chem.* 63 (1998) 7095; (b) T. Sakakura, J.-C. Choi, Y. Saito, T. Masuda, T. Sako, T. Oriyama, *J. Org. Chem.* 64 (1999) 4506.
- [2] J.-C. Choi, T. Sakakura, T. Sako, *J. Am. Chem. Soc.* 121 (1999) 3793.
- [3] See e.g.: (a) Y. Ono, *Appl. Catal. A* 155 (1997) 133. (b) *Chem. Br.* 30 (1994) 970. (c) *Eur. Chem. News* 21 (1998) 29.
- [4] As for the ^{119}Sn -NMR studies on $\text{Bu}_2\text{Sn}(\text{OPh})_2$, see: (a) P.J. Smith, R.F.M. White, L. Smith, *J. Organomet. Chem.* 40 (1972) 341. (b) J.D. Kennedy, *J. Chem. Soc. Perkin II* (1977) 242.
- [5] The formatin of $\text{Bu}_2\text{Sn}(\text{OPh})_2$ from $\text{Bu}_2\text{Sn}(\text{OMe})_2$ and phenol was briefly described, see: Ref. [4a].
- [6] H. Reuter, D. Schröder, *J. Organomet. Chem.* 455 (1993) 83.
- [7] A.M. Domingos, G.M. Sheldrick, *J. Chem. Soc. Dalton Trans.* (1974) 475.
- [8] H. Puff, H. Hevendehl, K. Höfer, H. Reuter, W. Schuh, *J. Organomet. Chem.* 287 (1985) 163.
- [9] V.B. Mokal, V.K. Jain, E.R.T. Tiekink, *J. Organomet. Chem.* 431 (1992) 283.
- [10] L. Pauling, *The Nature of the Chemical Bond*, third ed., Cornell University Press, Ithaca, NY, 1960, p. 224.
- [11] G.D. Smith, P.E. Fanwick, I.P. Rothwell, *Inorg. Chem.* 29 (1990) 3221.
- [12] (a) J. Holecek, M. Nadvornik, K. Handlir, A. Lycka, *J. Organomet. Chem.* 315 (1986) 299; (b) P.J. Smith, L. Smith, *Inorg. Chim. Acta Rev.* 7 (1973) 11; (c) B. Wrackmeyer, in: G.A. Webb (Ed.), *Annual Reports on NMR Spectroscopy*, vol. 16, Academic Press, Orlando, FL, 1985, p. 73.
- [13] A.J. Bloodworth, A.G. Davies, S.C. Vasishtha, *J. Chem. Soc. C* (1967) 1309.
- [14] D. Ballivet-Tkatchenko, O. Douteau, S. Stutzmann, *Organometallics* 19 (2000) 4563.
- [15] A.J. Bloodworth, A.G. Davies, *J. Chem. Soc.* (1965) 5238.
- [16] A.G. Davies, P.G. Harrison, *J. Chem. Soc. C* (1967) 1313.
- [17] (a) D.L. Alleston, A.G. Davies, *J. Chem. Soc.* (1962) 2050; (b) W. Gerrard, E.F. Mooney, R.G. Rees, *J. Chem. Soc.* (1964) 740.
- [18] W.J. Considine, J.J. Ventura, *J. Org. Chem.* 28 (1963) 221.